

Strain analysis in ultrathin silicide layers in Fe/CsCl-⁵⁷FeSi/Fe sandwiches

B. Croonenborghs,^{a)} F. M. Almeida, S. Cottenier, M. Rots,
A. Vantomme, and J. Meersschaut^{b)}

Instituut voor Kern- en Stralingsfysica, K.U. Leuven, Celestijnenlaan 200D, B-3001 Leuven, Belgium

(Received 26 February 2004; accepted 10 May 2004)

Epitaxially stabilized iron monosilicide films with the CsCl structure (B2-FeSi) have been investigated by conversion electron Mössbauer spectroscopy and x-ray diffraction. A detailed investigation of the elastic strain in these metastable layers is presented. Using hyperfine interaction information the tetragonal distortion of the silicide lattice could be quantified for layers as thin as 14 Å. A general tendency for strain relaxation with increasing layer thickness is observed. © 2004 American Institute of Physics. [DOI: 10.1063/1.1768307]

Almost all electronic devices rely on the proper functioning of often quite complex thin film and multilayer structures. The growth of a film on a substrate is generally associated with the build-up of large mechanical stresses. Consequently, the elastic energy of the system increases accordingly. Due to its possible detrimental effect on device performance, experimental investigations of intrinsic film strain and strain relaxation have a long tradition. Yet, it is important to realize that current electronic and magneto-electronic devices consist of multilayers where the individual layer thickness is only a few atomic layers.¹ The stress in such (sub)nanometer ultrathin films is no longer accessible via conventional strain analysis techniques such as x-ray diffraction (XRD) or Rutherford backscattering spectroscopy (RBS).

In this letter we describe an alternative approach to investigate the epitaxial strain, based on conversion electron Mössbauer spectroscopy (CEMS). This way a sensitivity close to the nanometer level can be reached. As an example, we present a detailed investigation of the epitaxial strain in metastable iron monosilicide films (B2-FeSi) embedded between two ferromagnetic iron layers. This system attracts considerable interest nowadays because of interlayer exchange coupling related phenomena.^{2,3} Using hyperfine interaction measurements the tetragonal distortion $\epsilon_T = \epsilon^{\parallel} - \epsilon^{\perp}$ of the lattice (where ϵ^{\parallel} and ϵ^{\perp} denote the strain parallel and perpendicular to the surface, respectively) could be quantified in silicide layers as thin as 14 Å.

Epitaxial Fe(80 Å)/⁵⁷FeSi/Fe(40 Å) sandwiches are grown with molecular beam epitaxy on polished MgO(001) substrates held at 150 °C. The pressure during growth was below 4×10^{-10} Torr. The iron constituting the ferromagnetic boundary layers has the natural isotopic composition whereas for the silicide layers Si is codeposited with isotopically enriched ⁵⁷Fe (95%). We used calibrated quartz crystal monitors to control the thickness, the deposition rate and the relative atomic flux. The deposition rates for ⁵⁷Fe and Si are 0.030 and 0.051 Å/s, respectively. The spacer thickness was varied from 8 to 165 Å. Finally, the samples were capped with 45 Å of Au, deposited at room temperature (RT), to prevent oxidation. Well-defined RHEED patterns are

maintained throughout the whole deposition sequence and indicate epitaxial growth.

XRD measurements were obtained using Cu K α radiation ($\lambda = 1.5415$ Å). Low angle $2\theta/\omega$ -scans (not shown) on samples with silicide thicknesses smaller than 30 Å exhibit clear oscillations up to $2\theta = 16^\circ$, indicative for very small thickness fluctuations. In Fig. 1 a set of CsCl-FeSi(001) Bragg peaks is shown. This diffraction is forbidden for the Fe layers (bcc structure) and, as a consequence, allows an accurate experimental determination of the silicide lattice parameter perpendicular to the surface. For the 165-Å-thick silicide layer the center of the diffraction peak is at $2\theta = 32.40(1)^\circ$, corresponding to an interplanar distance of 2.763(1) Å. The crystalline coherence length extracted from the peak width is around 140 Å. With decreasing film thicknesses, the peak position shifts to higher angles, indicating that the perpendicular lattice parameter decreases. Theoretical calculations^{4,5} as well as experimental results on completely relaxed films⁶ yield a lattice parameter of 2.77 Å. This indicates that the silicide layers are strained in tension. For spacers thinner than 50 Å it becomes impossible to determine the interplanar distance from XRD measurements.

Mössbauer spectroscopy has, due to its high sensitivity to the atomic and electronic surroundings of the Mössbauer probe ⁵⁷Fe, been successfully utilized in the study of epitax-

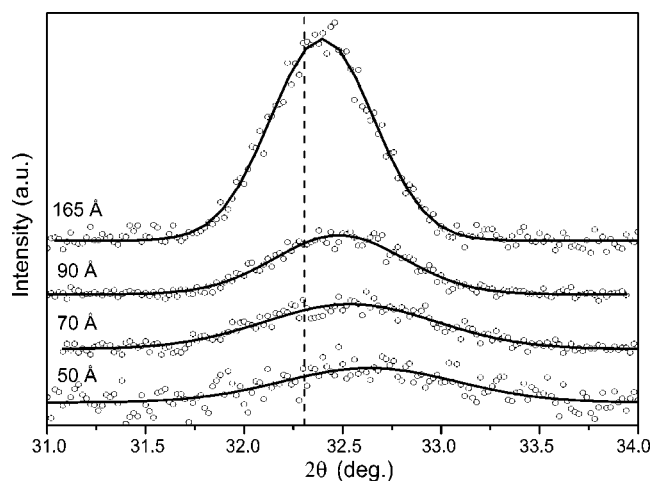


FIG. 1. $2\theta/\omega$ -scans of the FeSi(001) planes in case of a 165-, 90-, 70-, and 50-Å-thick spacer. The different spectra are shifted vertically for clarity. The dashed line at 32.31° indicates the location of the (001) diffraction for fully relaxed CsCl-FeSi, whereas the solid lines are Gaussian fits of the data.

^{a)}Electronic mail: bart.croonenborghs@fys.kuleuven.ac.be

^{b)}Electronic mail: johan.meersschaut@fys.kuleuven.ac.be

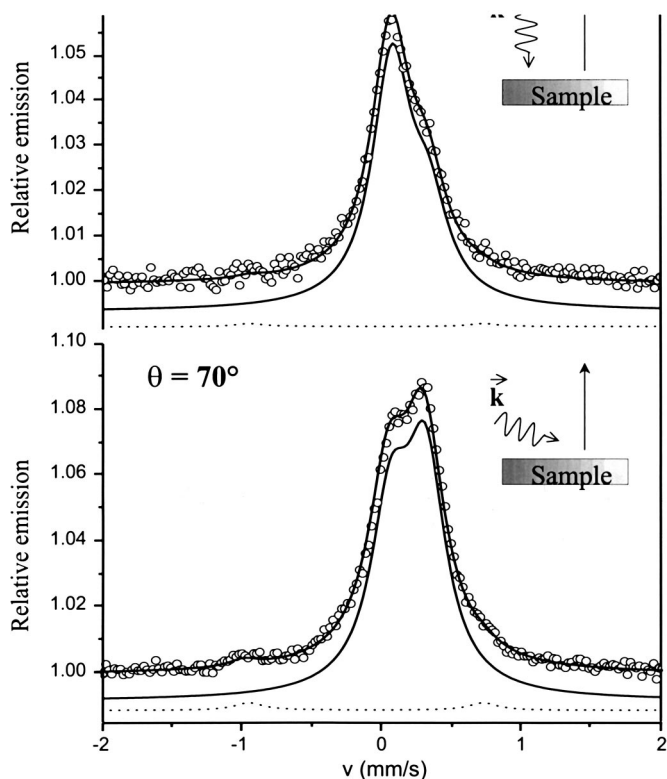


FIG. 2. Room temperature CEMS spectra of Fe(80 Å)/⁵⁷FeSi(30 Å)/Fe(40 Å) at two different angles θ between the incoming γ -ray direction and the normal to the surface of the sample. The two subspectra are displayed at the bottom of each spectrum. Due to selective ⁵⁷Fe enrichment, the dominating contribution (solid line) comes from the silicide layer.

ial phases of the Fe–Si system.^{7–9} Here it is used to investigate the epitaxial strain in ultrathin iron monosilicide layers with a metastable CsCl structure. CEMS measurements were performed at RT using a 12 mCi ⁵⁷Co in a Rh matrix source that was moved by a constant acceleration drive. The samples were incorporated as electrodes in a proportional gas detector. The resulting spectra obtained on a sample with nominal composition Fe(80 Å)/⁵⁷FeSi(30 Å)/Fe(40 Å) at two values of the angle θ between the γ direction and the normal to the sample are shown in Fig. 2. Consistent fits (solid lines through the data points) include a small component (dotted line) with the hyperfine parameters of α -Fe and a linewidth of 0.24 mm/s due to the presence of 2.25 at.% of ⁵⁷Fe nuclei in the natural iron layers. Because of the low velocity range of the depicted measurements, only two out of six possible nuclear transitions characteristic for bulk iron can be observed. We verified that CEMS measurements performed with a higher maximum velocity contain all six resonances and that the relative line intensities are in agreement with an in-plane orientation of the magnetization of the iron layers. For the silicide layer only one asymmetric doublet is taken into account. Due to the selective ⁵⁷Fe enrichment in the silicide layer, this is the dominating part of the spectrum (solid line). No fractions of other silicide phases or of interface components were observed. As fitting parameters only the isomer shift (δ), the quadrupole splitting (Δ), the linewidth (Γ), and the intensity ratio of the quadrupole components are used. The results are collected in Table I.

The CsCl structure is a simple cubic lattice with a basis of Fe at the origin and Si at (1/2, 1/2, 1/2). Due to this

TABLE I. Hyperfine parameters for the silicide component of the spectra in Fig. 2. The uncertainties on the last digit are as determined by the NORMOS analysis program (Ref. 15). The isomer shifts are given relative to α -Fe at room temperature.

Site	Parameter	$\theta=0^\circ$	$\theta=70^\circ$
FeSi	δ (mm/s)	0.31(2)	0.29(2)
	Δ (mm/s)	-0.26(1)	-0.25(1)
	Γ (mm/s)	0.33(1)	0.34(1)
	I_π/I_σ	2.7(1)	0.78(2)

symmetry, no quadrupole interaction is expected and as the monosilicide phase is nonmagnetic¹⁰ a single line spectrum should be observed. Due to strain-induced symmetry reduction however, a small electric field gradient (EFG) originates at the ⁵⁷Fe nucleus. In case of (001) oriented growth its principal axis (V_{zz}) is parallel to the [001] direction. In general, for a thin single-crystalline sample with a well-defined direction of the EFG, the ratio of the intensity of the two transitions $I_{1/2} \rightarrow I_{3/2} (\equiv I_\pi)$ and $I_{1/2} \rightarrow I_{1/2} (\equiv I_\sigma)$ of a quadrupole doublet is angular dependent. If the asymmetry parameter η is zero and the Lamb–Mössbauer factor is isotropic, one has¹¹

$$\frac{I_\pi}{I_\sigma} = \frac{3(1 + \cos^2\theta)}{5 - 3\cos^2\theta}, \quad (1)$$

where θ is the angle between the direction of the exciting photon and the principal axis of the electric field gradient. This dependence has been successfully used to characterize the EFG at the two iron sites in both α -FeSi₂ (Ref. 12) and β -FeSi₂.¹³ In Fig. 2 the angular dependence of the quadrupole components can be clearly identified and is consistent with an EFG of which the principal axis lies along the normal to the sample surface. Changing the angle θ from 0° to 70°, the ratio of the intensities of the line at higher and lower energy increases. This indicates a negative sign of the principal value of the EFG.¹¹ A similar behavior was found for all other samples with a spacer thickness larger than or equal to 14 Å.

Experimentally, for silicide layers thicker than or equal to 50 Å a linear correlation with a proportionality constant of -18.5(9)%/(mm/s) is obtained between the quadrupole splitting determined via CEMS and the tetragonal distortion determined by XRD. Extrapolation of this behavior to the thin silicide region (<50 Å), not accessible via XRD or RBS, is justified by the linear dependence of the quadrupole splitting with varying strain, as evidenced by *ab initio* calculations (not shown). Consequently, the extrapolation provides a straightforward way to determine the tetragonal distortion of the silicide lattice from the experimentally accessible hyperfine interaction parameters. The result is presented in Fig. 3. A clear relaxation process typical for lattice-mismatched epitaxial systems is identified. For such heterostructures, if the thickness of the layer is thinner than a critical thickness, coherent growth with the substrate is achieved. However, if the film thickness exceeds this critical thickness, the introduction of misfit dislocations near the interface is energetically favored. The strain relief by these interfacial defects has been discussed in detail by Matthews and Blakeslee.¹⁴ Since, to the best of our knowledge, no information is available about the nature of the dislocations formed in the Fe/CsCl-FeSi/Fe system, only a qualitative fit could be ob-

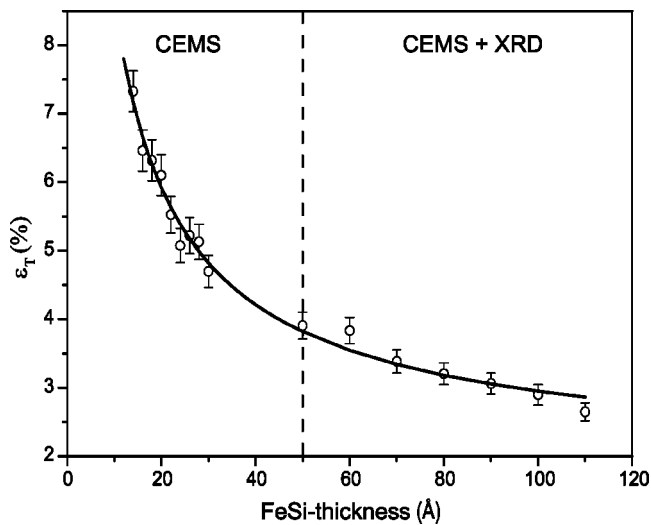


FIG. 3. Tetragonal distortion $\epsilon_T = \epsilon^{\parallel} - \epsilon^{\perp}$ of the monosilicide as a function of its thickness. The solid line is a fit using the strain relief mechanism described by Matthews and Blakeslee, whereas the dashed line indicates the thickness limit accessible via XRD.

tained employing their model (solid line in Fig. 3). It can be estimated from Fig. 3 that coherent growth is not achieved for monosilicide layers with a thickness down to at least 16 Å.

In conclusion, by combining conversion electron Mössbauer spectroscopy and x-ray diffraction, the epitaxial strain in the silicide layer of Fe/CsCl-⁵⁷FeSi/Fe sandwiches could be quantified down to thicknesses as low as 14 Å. A general tendency for strain relaxation with increasing layer thickness was observed. The approach introduced is not limited to the FeSi system, as illustrated here, but can be applied to other structures as well. We expect it to be also applicable to systems with a noncubic $L1_0$ crystal structure exhibiting a large perpendicular magnetic anisotropy such as Fe/Au, Fe/Pt,

and Fe/Pd. Here, the anisotropic electronic charge distribution will be reflected by asymmetrical line positions in the Zeeman sextet.¹¹

This work was supported by the F.W.O.-Vlaanderen Project Nos. G.0498.04 and G.0194.00, IUAP P5/1 and GOA(KULeuven). J.M. and S.C. thank the Belgian National Science Foundation (F.W.O.-Vlaanderen) for financial support.

¹J. Daughton, A. Pohm, R. Fayfield, and C. Smith, *J. Phys. D* **32**, R169 (1999).

²J. de Vries, J. Kohlhepp, F. den Broeder, R. Coehoorn, R. Jungblut, A. Reinders, and W. de Jonge, *Phys. Rev. Lett.* **78**, 3023 (1997).

³R. Gareev, D. Bürgler, M. Buchmeier, D. Olligs, R. Schreiber, and P. Günberg, *Phys. Rev. Lett.* **87**, 157202 (2001).

⁴H. von Känel, M. Mendik, K. Mäder, N. Onda, S. Goncalves-Conto, C. Schwarz, G. Malegori, L. Miglio, and F. Marabelli, *Phys. Rev. B* **50**, 3570 (1994).

⁵E. Moroni, W. Wolf, J. Hafner, and R. Podloucky, *Phys. Rev. B* **59**, 12860 (1999).

⁶N. Onda, H. Siringhaus, S. Goncalves-Conto, C. Schwarz, S. Zehnder, and H. von Känel, *Appl. Surf. Sci.* **73**, 124 (1993).

⁷M. Fanciulli, G. Weyer, A. Svane, N. Christensen, H. von Känel, E. Müller, N. Onda, L. Miglio, F. Tavazza, and M. Celino, *Phys. Rev. B* **59**, 3675 (1999).

⁸S. Degroote, A. Vantomme, J. Dekoster, and G. Langouche, *Appl. Surf. Sci.* **91**, 72 (1995).

⁹J. Desimoni and F. Sanchez, *Hyperfine Interact.* **122**, 277 (1999).

¹⁰D. Berling, G. Gewinner, M. Hanf, K. Hricovini, S. Hong, B. Loegel, A. Mehdaoui, C. Pirri, M. Tuilier, and P. Wetzel, *J. Magn. Magn. Mater.* **191**, 331 (1999).

¹¹V. Goldanskii and R. Herber, *Chemical Applications of Mössbauer Spectroscopy* (Academic, New York, 1968).

¹²H. Reuther, G. Behr, and A. Teresiak, *J. Phys.: Condens. Matter* **13**, L225 (2001).

¹³M. Fanciulli, C. Rosenblad, G. Weyer, A. Svane, and N. Christensen, *Phys. Rev. Lett.* **75**, 1642 (1995).

¹⁴J. Matthews and A. Blakeslee, *J. Cryst. Growth* **27**, 118 (1974).

¹⁵R. Brand, NORMOS programs version 1990.